INTERNATIONAL ATOMIC ENERGY AGENCY
UNITED NATIONS EDUCATIONAL, SCIENTIFIC AND CULTURAL ORGANIZATION
INTERNATIONAL CENTRE FOR THEORETICAL PHYSICS
I.C.T.P., P.O. BOX 586, 34100 TRIESTE, ITALY, CABLE CENTRATOM TRIESTE

H4-SMR 393/49

SPRING COLLEGE ON PLASMA PHYSICS

15 May - 9 June 1989

MAGNETOHYDRODYNAMICS:
STABILITY OF LARGE ASPECT RATIO TOKAMAKS

A. Bondeson

Ecole Polytechnique Federale de Lausanne
Av. des Bains
CH-1007 Lausanne
Switzerland

MAGNETOHYDRODYNAMICS: STABILITY OF LARGE ASPECT RATIO TOKAMAKS

A. Bondeson

Centre de Recherces en Physique des Plasmas
Association EURATOM - Confédération Suisse
Ecole Polytechnique Fédérale de Lausanne
Av. des Bains, CH-1007 Lausanne, Switzerland

Abstract: An introduction to magnetohydrodynamics (MHD) is given, aimed at describing the stability of tokamaks in the cylindrical approximation. The lowest-order reduced-MHD equations are derived and analyzed for the stability of external kink and resistive tearing modes. The resistive layer problem for the tearing mode is solved by means of Fourier transformation. Finally, a brief overview is given of nonlinear results, including computational results for major disruptions in tokamaks.

1. INTRODUCTION: THE MAGNETOHYDRODYNAMIC EQUATIONS

Magnetohydrodynamics, where the plasma is treated as a single conducting and compressible fluid, is the most basic description of the macroscopic behavior of a plasma. MHD finds many applications in astrophysical and geophysical contexts, but over the past 30 - 35 years, much of the impetus for development of the theory has come from nuclear fusion research and the need to understand and control various devices for magnetic confinement of plasma. For such schemes, principally tokamaks, stellarators, and reversed field pinches (RFP), MHD theory and computation is used to describe the most prominent motions of the plasma, occurring on fast time-scales and large spatial scales. A relatively detailed agreement exists between MHD predictions and the experimentally observed behavior of these devices. Most importantly, MHD (sometimes in combination with other theories) predicts operational limits to plasma current, pressure, and density, all of which limit performance of the respective configurations, and is therefore essential for the optimal design and construction of future experiments.

MHD treats the plasma as an ideal gas with electrical resistivity η, acted upon by the volume Lorentz force $\mathbf{J} \times \mathbf{B}$. These equations can be written down directly,

$$\rho\left(\frac{\partial \mathbf{v}}{\partial t} + \mathbf{v}\cdot\nabla\mathbf{v}\right) = \mathbf{J} \times \mathbf{B} - \nabla p \tag{1.1}$$

$$\mu_0 \mathbf{J} = \nabla \times \mathbf{B} \tag{1.2}$$

$$\mathbf{E} + \mathbf{v} \times \mathbf{B} = \eta \mathbf{J} \tag{1.3}$$

$$\frac{\partial \mathbf{B}}{\partial t} = -\nabla \times \mathbf{E} = \nabla \times (\mathbf{v} \times \mathbf{B} - \eta \mathbf{J}) \tag{1.4}$$

$$\frac{\partial \rho}{\partial t} + \nabla\cdot(\rho \mathbf{v}) = 0 \tag{1.5}$$

$$\frac{\partial p}{\partial t} + \mathbf{v}\cdot\nabla p + \gamma p\, \nabla\cdot\mathbf{v} = 0 \tag{1.6}$$

Equation (1.2) is the pre-Maxwell form of Ampère's law, where the displacement current is ignored. This is a good approximation as long as the characteristic wave speed, the Alfvén speed $v_A = B/(\mu_0\rho)^{1/2}$, satisfies $v_A^2 << c^2$. In the MHD equations (1.1-6), two assumptions are made, that are not trivially satisfied in many plasmas of interest. The first is the assumption of a scalar pressure evolving in time according to the adiabatic law (1.6), where one conventionally sets $\gamma = 5/3$. A rigorous derivation of (1.6) for a plasma can be given only if we consider processes slower than the ion-ion collision time. This time-scale is of the order of several milliseconds in present-day tokamaks, that is, much longer than the characteristic Alfvén time $\tau_A = R/v_A$, where R denotes the major radius. Despite this, in many cases of interest, the hydrodynamic equation (1.6) is valid. This is to some extent because many important MHD phenomena are incompressible and the pressure is simply convected with the fluid. Under these circumstances, the value of γ is unimportant. In other cases, such as for example the description of ion-acoustic waves[1] or the equilibrium[2] and stability[3] of plasmas with mass flows, Eq. (1.6) has to be replaced by a more accurate (and more complicated) description that takes into account the free-streaming of particles along the magnetic field lines.

The other weak point of MHD is the assumption of an Ohm's law in the form $\mathbf{E} + \mathbf{v} \times \mathbf{B} = \eta \mathbf{J}$. This form is easily justified for conducting liquids, e.g., mercury or melted iron. However, if we attempt to derive (1.3) for a plasma by subtracting the equations of motion for electrons and ions, we find two additional terms, $\mathbf{E} + \mathbf{v} \times \mathbf{B} = \eta \mathbf{J} + (\mathbf{J} \times \mathbf{B} - \nabla p_e)/ne$, where $\mathbf{J} \times \mathbf{B}/ne$ is referred to as the Hall term and $\nabla p_e/ne$ as the electron diamagnetic drift term. These terms can be shown to be negligible if we limit consideration to not too fast phenomena (frequencies much less than the ion gyro-frequency $\Omega_i = eB/m_i$) and scale lengths larger than the ion Larmor radius $\rho_i = v_{thi}/\Omega_i$. MHD can be looked at as the limit where the mass density and velocity, magnetic field and electrical current are finite, but where the electrical charge density of either species $n_e e$ is "large". This immediately tells us that the term $(\mathbf{J} \times \mathbf{B} - \nabla p_e)/ne$ can be dropped. It also shows that MHD effectively sets the electron and ion velocities equal, although $\mathbf{J} = ne(\mathbf{v}_i - \mathbf{v}_e)$ is nonzero.

It is clear that the strength of MHD, and the reason for its success is not the detailed description of all possible types of plasma behavior, but rather that it is a simple set of equations, that allows solution even in rather complicated geometries and for various plasma

profiles. It is usually a good approximation on time scale from a fraction to several thousands of an Alfvén time, and space scales larger than the ion Larmor radius. A more detailed discussion of the validity of the MHD equations is given in the excellent review article by J. Freidberg [4]. An important property of the MHD equations is that they have certain nice mathematical properties, that have made possible a detailed analysis of the stability of various configurations.

Before entering a discussion of MHD, one remark has to be made. Over 30 years of research in this subject has created an enormous body of results. It is obviously impossible to survey this subject in a few lectures, and such a task would be far beyond my ability. Rather, I have tried to discuss certain aspects that are simple, but basic and important, in particular for the stability of tokamaks.

2. SOME GENERAL PROPERTIES OF IDEAL MHD

A. Lagrangian form of ideal MHD

For sufficiently short time-scales, the resistive electric field $\eta\mathbf{J}$ can be neglected in Ohm's law and we are left with the ideal MHD system,

$$\rho \frac{d\mathbf{v}}{dt} = \mathbf{J}\times\mathbf{B} - \nabla p \tag{2.1}$$

$$\frac{d\mathbf{B}}{dt} = \mathbf{B}\cdot\nabla\mathbf{v} - \mathbf{B}\nabla\cdot\mathbf{v} \tag{2.2}$$

$$\frac{d\rho}{dt} + \rho\,\nabla\cdot\mathbf{v} = 0 \tag{2.3}$$

$$\frac{dp}{dt} + \gamma p\,\nabla\cdot\mathbf{v} = 0 \tag{2.4}$$

Here, the total time derivative $d/dt = \partial/\partial t + \mathbf{v}\cdot\nabla$ has been used consistently to simplify a Lagrangian description. In the Lagrangian description, one identifies fluid elements, that are displaced from some reference position $\mathbf{x}$ at time $t = 0$ to $\mathbf{y}(\mathbf{x},t) = \mathbf{x} + \xi(\mathbf{x},t)$ at some later time t. The dependent variables ρ, p and $\mathbf{B}$ are then considered functions of the *original* position $\mathbf{x}$ and time, rather than of the *present* position $\mathbf{y}$ and time as in the Eulerian description; thus, for example, $\rho_L(\mathbf{x},t) = \rho_E(\mathbf{y}(\mathbf{x},t),t)$.

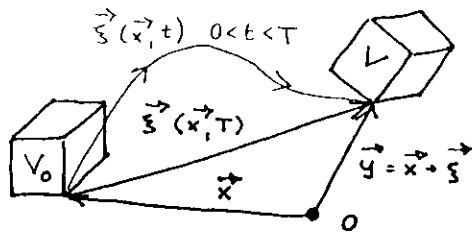

Figure 1. Original and displaced volume element

An important quantity is the Jacobian, or the ratio of volume elements in the displaced and original position,

$$J = \frac{V}{V_0} = \frac{d^3y}{d^3x} = \mathrm{Det}\left(\frac{\partial y_i}{\partial x_j}\right) = \frac{\partial \mathbf{y}}{\partial x_1}\cdot\left(\frac{\partial \mathbf{y}}{\partial x_2}\times\frac{\partial \mathbf{y}}{\partial x_3}\right) \tag{2.5}$$

Conservation of mass can be written as

$$\rho(\mathbf{x},t) = \rho_0(\mathbf{x}) / J(\mathbf{x},t) \tag{2.6}$$

or, shorter

$$\rho = \rho_0 / J \tag{2.6'}$$

Furthermore, the expansion rate of a volume element is

$$\frac{1}{J}\frac{dJ}{dt} = \nabla\cdot\mathbf{v}$$

and thus (2.4) gives

$$p = p_0 / J^{\gamma} \tag{2.7}$$

Finally, it is easy to show by direct substitution that the ideal MHD evolution equation (2.2) for the magnetic field is satisfied by

$$\mathbf{B} = \frac{1}{J}\,\mathbf{B}_0\cdot\nabla_x\mathbf{y} \quad , \text{ or } \quad B_i = \frac{1}{J}\,B_{0j}\frac{\partial y_i}{\partial x_j} \tag{2.8}$$

i.e., except for a factor 1/J, the magnetic field transforms the same way as a line element

$$d\mathbf{y} = d\mathbf{x}\cdot\nabla_x\mathbf{y} \quad , \text{ or } \quad dy_i = dx_j\frac{\partial y_i}{\partial x_j} \tag{2.9}$$

This means that two fluid elements, initially on the same field line will always remain on the same field line. Consequently, field lines are "frozen" into the plasma in ideal MHD, and cannot be broken by any continous deformation of the fluid. Another way to say this is that the magnetic field lines may be thought of as deformable, but unbreakable "wires". The topology of the configuration of wires cannot be changed in time, and this tends to make the ideal MHD plasma rigid. On sufficiently long time-scales, one has to consider the effect of resistivity, which allows field lines to break and reconnect.

Equations (2.6-8) show that the state of the displaced plasma is a function only of the instantaneous position, not of the time history of the system, i.e., the state does not depend on the route the plasma followed from $\mathbf{x}$ to $\mathbf{y}$. An interesting consequence of these explicit expressions is that it is also possible to formulate a potential energy, which is a function of the instantaneous coordinates and to formulate MHD as a Hamiltonian system. To see this, we first write down the Lagrangian as the difference between kinetic and potential energy

$$L \equiv \int \mathcal{L}\, d^3x = W_{kin} - W_{pot} \quad ,$$

$$W_{kin} = \int \tfrac{1}{2}\rho v^2 \, d^3y \quad , \qquad W_{pot} = \int \left(\frac{1}{2\mu_0}B^2 + \frac{p}{\gamma-1}\right) d^3y \tag{2.10}$$

The Lagrange density, in terms of the original coordinates, becomes

$$\mathcal{L} = \tfrac{1}{2}\rho_0 \dot{\xi}^2 - \left[\frac{1}{2\mu_0 J}(\mathbf{B}_0\cdot\nabla_x y)^2 + \frac{p_0}{\gamma-1}J^{1-\gamma}\right] \tag{2.11}$$

with $\mathbf{y} = \mathbf{x} + \xi$. Using $\partial J/\partial\xi_{i,j} = J\,\partial x_j/\partial y_i$ and $\partial/\partial x_j(\partial J/\partial\xi_{i,j}) = 0$, it is easy to verify that the Lagrangian equation of motion

$$\frac{d}{dt}(\partial\mathcal{L}/\partial\dot{\xi}_i) = \partial\mathcal{L}/\partial\xi_i - \frac{\partial}{\partial x_j}(\partial\mathcal{L}/\partial\xi_{i,j}) \tag{2.12}$$

reproduces the equation of motion (2.1) for the fluid elements. To construct the Hamiltonian, we define the momentum density

$$\pi_i = \partial\mathcal{L}/\partial\dot{\xi}_i = \rho_0\dot{\xi}_i \tag{2.13}$$

The Hamiltonian is obtained in the standard way,

$$\begin{aligned} H &\equiv \int \mathcal{H}\, d^3x = \int \pi\cdot\dot{\xi}\, d^3x - L \\ &= \int \frac{\pi^2}{2\rho_0}\, d^3x + \int \left[\frac{1}{2\mu_0 J}(\mathbf{B}_0\cdot\nabla_x y)^2 + \frac{p_0}{\gamma-1}J^{1-\gamma}\right] d^3x \end{aligned} \tag{2.14}$$

and the equation of motion can be written as

$$\begin{aligned} \frac{d\xi_i}{dt} &= \frac{\delta H}{\delta\pi_i} = \frac{\partial\mathcal{H}}{\partial\pi_i} \\ \frac{d\pi_i}{dt} &= -\frac{\delta H}{\delta\xi_i} = -\frac{\partial\mathcal{H}}{\partial\xi_i} + \frac{\partial}{\partial x_j}(\partial\mathcal{H}/\partial\xi_{i,j}) \end{aligned} \tag{2.15}$$

It may be noted that the potential energy in (2.10) does not contain the electric field energy. That is due to the neglect of the displacement current in Ampère's law.

B. Global conservation laws

We now consider an ideal-MHD plasma in a volume V, surrounded by a nonmoving, rigid, perfect conductor, in which $\mathbf{B} = 0$. The boundary conditions on the wall are $\hat{n}\times\mathbf{E} = 0$, $\hat{n}\cdot\mathbf{B} = 0$, and $\hat{n}\cdot\mathbf{v} = 0$, where $\hat{n}$ is the outward normal of the surrounding surface S. It is then easy to show the following global conservation laws

$$\frac{d}{dt}\int_V \rho\, d^3x = 0 \qquad \text{mass} \tag{2.16}$$

$$\frac{d}{dt}\int_V \rho v\, d^3x = -\oint_S \left(p + \frac{B^2}{2\mu_0}\right)\hat{n}\, dS \qquad \text{momentum} \tag{2.17}$$

$$\frac{d}{dt}\int_V \left(\frac{\rho v^2}{2} + \frac{p}{\gamma-1} + \frac{B^2}{2\mu_0}\right) d^3x = 0 \qquad \text{energy} \tag{2.18}$$

$$\frac{d}{dt}\int_V \tfrac{1}{2}\,\mathbf{A}\cdot\mathbf{B}\, d^3x = 0 \qquad \text{magnetic helicity} \tag{2.19}$$

where the integrals are now written in terms of Eulerian variables, and where A denotes the vector potential; $\mathbf{B} = \nabla\times\mathbf{A}$. The conservation of energy,

$$\begin{aligned} &W = W_{kin} + W_{pot} = \text{constant}\,, \\ &W_{kin} = \int_V \frac{\rho v^2}{2}\, d^3x\,, \qquad W_{pot} = \int_V \left(\frac{p}{\gamma-1} + \frac{B^2}{2\mu_0}\right) d^3x \end{aligned} \tag{2.20}$$

allows us to use an Energy Principle to determine the stability of the plasma. A given magnetic configuration (in which the plasma is at rest) is stable if its potential energy is at a minimum

with respect to all perturbations of the plasma, with p and B given by Eqs. (2.7-8). This follows from the energy conservation relation (2.20), simply because no potential energy can be released to produce kinetic energy. Therefore, the kinetic energy cannot grow, and exponential instability is excluded. This argument is the basis for stability analysis by the energy integral or δW metod, that is commonly used in ideal MHD.

The local conservation laws (2.6-8) may be considered as constraints for the evolution of the plasma. These local conservation laws can be integrated in space to produce global conservation laws, the most important of which are given in (2.16-19). An interesting way to generate very stable equilibria has been suggested and exploited, in astrophysical contexts by Woltjer [5], and in the context of fusion devices by J. B. Taylor[6]. The idea is that the ideal-MHD plasma will be stable if the potential energy is at a minimum with respect not only to the motions in which the pressure and magnetic field evolve according to (2.7) and (2.8), but to a broader class of motions, constrained only by some of *global* conservation laws. Of particular interest to fusion devices is the case when the total magnetic helicity (2.19) is fixed. Minimization of the potential energy with the magnetic helicity constrained leads to the Euler-Lagrange equation

$$\mathbf{J} = \lambda \mathbf{B} \qquad (2.21a)$$

$$\nabla p = 0 \qquad (2.21b)$$

$$\lambda = \text{constant} \qquad (2.21c)$$

Several devices for magnetic confinement are rather close to such "Taylor-states", e.g., reversed field pinches[7] and spheromaks[8]. However, the above minimization is, in a sense, too pessimistic. This is clear, not only from the derivation, where all the constraints implied by (2.7) and (2.8) are replaced by one single constraint (2.19), but also because it predicts relaxed states in which no pressure is magnetically confined. Computation of the maximum pressure that can be stably confined is an important application of MHD theory and computation, and one in which good correlation has been obtained between theory and experiment, at least for tokamaks[9].

3. LARGE ASPECT RATIO ORDERING

Despite the simple appearence of the ideal MHD system (2.1-4) the behaviour of its solutions is enormously complex, in fact, even the linear spectrum is rather complicated. Therefore, in these introductory lectures, we will be concerned with a simplified system, the socalled reduced MHD equations. Because of its simplicity this system has been a very popular tool in tokamak research over the past 15 years. It is useful because it gives a good description

of the two types of modes that set the most basic limitations on tokamak operation, namely, the external kink modes and resistive tearing modes. There are, of course, many aspects of tokamak stability that are not described by these equations. In particular, all pressure driven instabilities, which determine the maximum stable $\beta = 2\langle p\rangle/\mu_0\langle B^2\rangle$, are neglected in the system we will discuss here. However, ohmically heated tokamaks have β-values well below the stability limit, and it is only by the application of significant auxiliary heating that the β-limit can be reached.

A derivation of the "lowest order reduced MHD equations", given by H. Strauss[10] will be reproduced here. As a first step, we approximate the tokamak by a long thin cylinder with periodic boundary conditions, and assume that the aspect ratio R/a (where R is the major radius, and a the minor radius) is large, i.e., $\varepsilon = a/R << 1$.

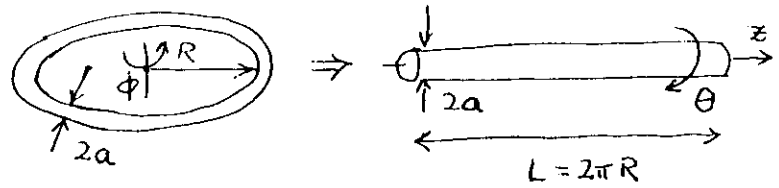

Figure 2. Cylindrical model of a large aspect ratio tokamak.

ε will be used as an expansion parameter and we first consider the order of magnitude of different quantities. Tokamaks are characterized by having the safety factor q, defined as the number of toroidal turns a field line makes in completing one poloidal turn ($=B_\phi r/B_\theta R$ in the cylindrical approximation) of order unity, i.e., $B_\phi/R \sim B_\theta/a$. Furthermore, the modes of importance in MHD show little variation along a field line $\mathbf{B}\cdot\nabla = B_z\partial/\partial z + \mathbf{B}_\perp\cdot\nabla_\perp \approx 0$. Here, $\perp$ stands for components in the poloidal (r,θ) plane. Thus, if we take the minor radius a and the toroidal field B_z to be of order unity, it follows that

$$\nabla_\perp \sim 1/a = O(1) \quad , \quad \partial/\partial z \sim 1/R = O(\varepsilon)$$
$$B_\perp = O(\varepsilon) \quad , \quad J_z = O(\varepsilon) \qquad (3.1a)$$

In addition to this, the lowest order reduced equations assume that the pressure is $O(\varepsilon^2)$, which also means that

$$J_\perp = O(\varepsilon^2) \qquad , \qquad B_z = \text{constant} + O(\varepsilon^2) \tag{3.1b}$$

As a consequence of this, $\mathbf{B}$ can be represented as

$$\mathbf{B} = \nabla\psi \times \hat{z} + B_z \hat{z} \tag{3.2}$$

[Note that the leading order terms in $\nabla \cdot \mathbf{B}$ vanish and that $\nabla \cdot \mathbf{B} = O(\varepsilon^3)$]. ψ is the z-component of the vector potential and is usually referred to as the poloidal flux function. Forces in the z-direction arise from $\mathbf{J}_\perp \times \mathbf{B}_\perp$, which is one order smaller in ε than forces in the poloidal plane, $J_z \hat{z} \times \mathbf{B}_\perp$. Thus, to lowest order, $\mathbf{v} = \mathbf{v}_\perp$ and $v_z = 0$. For the time evolution of the vector potential, it is useful to add a gauge potential,

$$\frac{\partial \mathbf{A}}{\partial t} = -\mathbf{E} + \nabla V = \mathbf{v} \times \mathbf{B} + \nabla V \tag{3.3}$$

To assure that the perturbed vector potential only has a z-component (as implicitly assumed in (3.2)), we now demand that

$$0 = \hat{z} \times \frac{\partial \mathbf{A}}{\partial t} = \hat{z} \times (\mathbf{v} \times \mathbf{B}) + \hat{z} \times \nabla V = v_\perp B_z - \nabla V \times \hat{z} \tag{3.4}$$

This gauge condition shows that $\phi \equiv V/B_z$ is the stream function for the plasma motion in the perpendicular plane

$$\mathbf{v}_\perp = \nabla\phi \times \hat{z} \tag{3.5}$$

and that to lowest order the motion is incompressible. The z-component of (3.3) becomes

$$\frac{\partial \psi}{\partial t} = \hat{z} \cdot (\mathbf{v}_\perp \times \mathbf{B}_\perp) + B_z \hat{z} \cdot \nabla\phi = \mathbf{B}_\perp \cdot \nabla_\perp \phi + B_z \hat{z} \cdot \nabla\phi$$
$$= \mathbf{B} \cdot \nabla\phi \tag{3.6}$$

The current density is

$$\mathbf{J} = \nabla \times (\nabla\psi \times \hat{z}) + \nabla B_z \times \hat{z} = -\nabla_\perp^2 \psi \, \hat{z} + \nabla_\perp \frac{\partial \psi}{\partial z} + \nabla B_z \times \hat{z} \tag{3.7}$$

From here on, we set $\mu_0 = 1$, as is common practice in MHD. This simply amounts to a redefinition of the magnetic field strength. Substituting (3.5) and (3.7) into the equation of motion (2.1) gives

$$\rho \frac{d}{dt} \nabla\phi \times \hat{z} = -\nabla_\perp \psi \nabla_\perp^2 \psi - B_z \hat{z} \times \nabla_\perp \frac{\partial \psi}{\partial z} - \nabla_\perp (p + B_z^2/2)$$

As usual, for incompressible motion, it is sufficient to consider the curl of the equation of motion. The z-component of the curl gives an evolution equation for the vorticity

$$\rho \left(\frac{\partial}{\partial t} + \mathbf{v}_\perp \cdot \nabla\right) \nabla_\perp^2 \phi = \mathbf{B}_\perp \cdot \nabla_\perp \nabla_\perp^2 \psi + B_z \frac{\partial}{\partial z} \nabla_\perp^2 \psi$$
$$= \mathbf{B} \cdot \nabla \nabla_\perp^2 \psi \tag{3.8}$$

where we assumed that the mass density is constant in space. It is useful to introduce the z-component of the vorticity and electrical current density as auxiliary variables

$$\omega = -\nabla_\perp^2 \phi \qquad , \qquad j = -\nabla_\perp^2 \psi \tag{3.9}$$

The reduced MHD equations can now be written in a compact form,

$$\rho \left(\frac{\partial}{\partial t} + \mathbf{v}_\perp \cdot \nabla\right) \omega = \mathbf{B} \cdot \nabla j \tag{3.10a}$$

$$\frac{\partial \psi}{\partial t} = \mathbf{B} \cdot \nabla\phi \tag{3.10b}$$

The simplification from the full MHD system is evident; instead of the six vector components $\mathbf{v}$ and $\mathbf{B}$ and two scalars ρ and p, we now only have two scalars ϕ and ψ to evolve in time. ϕ is evolved in time by evolving ω according to (3.10a) and inverting Laplace's equation $\nabla_\perp^2 \phi = -\omega$ with the appropriate boundary conditions.

Of course, the nonlinear system (3.10) has an energy integral

$$W = W_{kin} + W_{mag} = \text{constant}, \quad W_{kin} = \int \frac{\rho}{2} (\nabla_\perp \phi)^2 \, d^3x = \int \frac{\rho}{2} v_\perp^2 \, d^3x \, ,$$
$$W_{mag} = \int \frac{1}{2} (\nabla_\perp \psi)^2 \, d^3x = \int \frac{1}{2} B_\perp^2 \, d^3x \, , \tag{3.11}$$

which means that the Energy Principle[11] can be used to study the stability. If a given configuration has the magnetic potential energy at a minimum, then it is stable, if not, it is unstable.

The system (3.10) is the lowest order approximation in $\epsilon = a/R$ of MHD in a tokamak. Approximations in increasing orders in ϵ have been given by Strauss[12], Drake and Antonsen[13] and Izzo et al[14]. Maschke and Morros Tosas[15] show how these approximations can be derived from an exact formulation of MHD in terms of stream functions and potentials.

4. IDEAL LINEAR THEORY IN A CYLINDER

To proceed we assume that the equilibrium has cylindrical symmetry $j_0 = j_0(r)$, $\partial/\partial\theta = \partial/\partial z = 0$. The equilibrium relation is then simply

$$j_0 = -\frac{1}{r}\frac{d}{dr} r \frac{d\psi_0}{dr} \tag{4.1}$$

We assume an $\exp(i\omega t + im\theta - inz/R)$ dependence for the perturbed quantities, where m is the poloidal mode number and n the toroidal mode number (z/R being the cylindrical equivalent of the toroidal angle). Linearization of the reduced MHD equations (3.10) gives

$$\begin{aligned} &\omega\psi = F\phi \\ &\rho\omega\left(\frac{1}{r}\frac{d}{dr} r \frac{d\phi}{dr} - \frac{m^2}{r^2}\phi\right) = F\left(\frac{1}{r}\frac{d}{dr} r \frac{d\psi}{dr} - \frac{m^2}{r^2}\psi\right) - \frac{m}{r}\frac{dj_0}{dr}\psi \end{aligned} \tag{4.2}$$

where

$$F = \mathbf{k}\cdot\mathbf{B} = mB_\theta/r - nB_z/R = \frac{B_z}{R}\left(\frac{m}{q} - n\right) \tag{4.3}$$

For the purpose of an ideal MHD stability analysis, it is useful to introduce $U = \phi/\omega$ which is a stream function for the displacement, so that $\psi = FU$. Multiplying (4.2) by U and integrating by parts, we obtain the square of the eigenfrequency as a Rayleigh quotient

$$\omega^2 = -\gamma^2 = \delta W / K \tag{4.4a}$$

Here γ denotes the growth-rate,

$$K = \frac{1}{2}\int_0^a \rho\left[\left(\frac{dU}{dr}\right)^2 + \frac{m^2}{r^2}U^2\right] r dr \tag{4.4b}$$

represents inertia and

$$\delta W = \frac{1}{2}\int_0^\infty \left[\left(\frac{d\psi}{dr}\right)^2 + \frac{m^2}{r^2}\psi^2 + \frac{m}{B_\theta(m-nq)}\frac{dj_0}{dr}\psi^2\right] r dr \tag{4.4c}$$

represents the magnetic potential energy of the perturbation. Instability results if, and only if, there is a perturbation that makes $\delta W < 0$.

δW in (4.4c) contains two positive definite terms, and there is only one, proportional to the current gradient, that can cause instability. We note that the Taylor state $\mathbf{J} = \lambda\mathbf{B}$, in the large aspect ratio limit, has j = constant and therefore has removed this source of energy. However, in order to have j = constant *everywhere*, it is necessary to have a conducting wall right on the plasma. In the next subsection, we shall consider the stability of external modes, when such a wall is either absent or separated from the plasma.

A. External modes

We now consider external modes that do not have a resonant surface inside the plasma, in other words $F \neq 0$ and $q \neq m/n$ everywhere in the plasma. In this case we can use arbitrary trial functions for ψ in δW. (If the resonant surface q = m/n is located inside the plasma, ideal MHD requires that the perturbed magnetic flux ψ vanish on the resonant surface, since $U = \psi/F$. A 1/x singularity of U would make $K = \infty$ and therefore $\omega^2 = 0$.)

For simplicity, we consider the "top-hat" current distribution of Shafranov[16], where the current is flat inside the plasma and falls discontinuously to zero at the plasma-vacuum boundary

$$j_0 = 2B_z/Rq_0 \quad \text{for} \quad r < a, \quad \text{and} \quad j_0 = 0 \quad \text{for} \quad r > a\,. \tag{4.5}$$

A simple way to find an appropriate test function for ψ in δW is to solve the corresponding Euler-Lagrange equations for δW stationary separately in the two regions $r < a$ and $r > a$, and join the two solutions at r =a. The Euler-Lagrange equation is

$$\frac{1}{r}\frac{d}{dr} r \frac{d\psi}{dr} - \frac{m^2}{r^2}\psi - \frac{m}{B_\theta(m-nq)}\frac{dj_0}{dr}\psi = 0 \tag{4.6}$$

For the top-hat profile where $dj_0/dr = 0$ everywhere except at r=a, the appropriate solutions of (4.6) are $\psi = (r/a)^m$ for $r < a$ and $\psi = (r/a)^{-m}$ for $r > a$. Here, we have assumed that m is positive and that there is no conducting wall in the external region. Substituting these solutions into δW (most easily done after an integration by parts) we obtain

$$\delta W = \frac{a}{2}\,\psi_a\,(\psi_-' - \psi_+') - \frac{m}{m - nq_0}\,\psi_a^2 = m\left(1 - \frac{1}{m - nq_0}\right)\psi_a^2 \qquad (4.7)$$

Equation (4.7) shows that instability occurs if and only if

$$0 < m - nq_0 < 1 \qquad (4.8a)$$

or, (assuming $n > 0$) for q_0 in the range

$$(m-1)/n < q_0 < m/n \qquad (4.8b)$$

We see from (4.8a) that for every toroidal mode number n there is at least one poloidal mode number m for which this profile is marginal or unstable. This is not very surprising, since the sharp current gradient of the top-hat profile is somewhat unrealistic, and is very effective in creating instability for high m. A rounded off profile is more stable for large m, and for realistic current profiles it is only stability to m = 1, 2 and 3 that is critical. However, an interesting aspect of the top-hat profile is that for q_0 integer, there is *no* mode that is unstable, only marginal modes with $m = nq_0$ and $m = nq_0 + 1$.

A powerful way to increase the stability to these external modes is to introduce a perfectly conducting wall. We let the wall be positioned at $r = b > a$. In this case, the external solution of (4.6) must satisfy $\psi(b) = 0$, thus

$$\psi = \frac{(b/r)^m - (r/b)^m}{(b/a)^m - (a/b)^m} \qquad , \qquad r > a \qquad (4.9)$$

The region for instability becomes

$$(1/n)\,|\,m - 1 + (a/b)^{2m}\,| < q_0 < m/n \qquad (4.10)$$

and the unstable range of q_0 has been reduced by a factor $1 - (a/b)^{2m}$. If the wall is right on the plasma boundary, b = a, there is no instability at all. Typically, tokamaks have conducting walls with $b/a \geq 1.15$. As the effect of the wall is proportional to $(a/b)^{2m}$, wall stabilization is powerful only for low m. Furthermore, in reality, walls only have finite conductivity, and can only stabilize the external modes over a certain time-scale.

We now consider the case where the region of nonzero current only occupies part of the cross-section $r < r_c$, with $r_c < a$. Outside this region q increases with the radius as $q(r) = q_0(r/r_c)^2$, and at the plasma boundary, $q_a = q(a) = q_0(a/r_c)^2$. If $q_a < m/n$, there is no resonant surface in the plasma and the condition for instability is unchanged (4.8) or (4.10). However, if the resonant q-value m/n lies between q_0 and q_a, then the resonant surface where F = 0 is located within the plasma, and the test function for ψ has to be zero at the resonant surface.

This has the important consequence that the ideal mode with mode numbers m and n is stable, as can be seen by rewriting δW in terms of $\xi = U/r$, proportional to the radial displacement

$$\delta W = \frac{1}{2}\int_0^a |\, r^2F^2\xi'^2 + (m^2-1)F^2\xi^2 \,|\, r\,dr \;-\; \frac{1}{2}\,|\,r^3F^2\Delta + (m^2-n^2q^2)\,B_\theta^2\,|_{r=a}\,\xi_a^2 \qquad (4.11)$$

In (4.11) it is assumed that the equilibrium current vanishes at r=a. The contribution to δW from the vacuum region $a < r < b$ is contained in the term proportional to

$$\Delta = \psi'/\psi|_{r=a} = -\frac{m}{a}\,\frac{1 + (a/b)^{2m}}{1 - (a/b)^{2m}} \qquad (4.12)$$

If $n^2q_a^2 > m^2$, *all* terms in (4.11) are positive definite for $m > 1$, and semidefinite for $m = 1$. Thus, all $m > 1$ modes are *stable* when $n^2q_a^2 > m^2$, independent of the current profile.

It is now easy to work out the ideal stability for the Shafranov equilibrium in terms of q_0 and q_a. It is unstable to the (m,n) mode if, and only if,

$$q_a < m/n \qquad (4.13a)$$

and the potential energy (4.7) is negative,

$$(m-1)/n < q_0 < m/n \qquad (4.13b)$$

In order to construct a stability diagram, one must consider the condition (4.13) for all positive m and n. It turns out that the most stringent conditions are set by n = 1 and the stability diagram takes the following shape

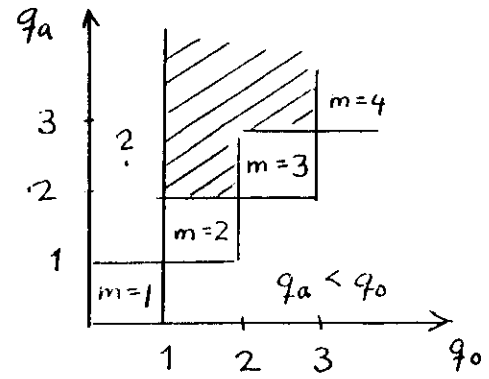

Figure 3. Ideal-MHD stability diagram for the Shafranov current profile. The dashed region is stable.

The dashed region is stable and the boxes are unstable to an n=1 mode with poloidal modenumber as marked in each box. In the region marked by a question mark, there is a marginally stable m=1/n=1 mode, whose displacement is nonzero and constant inside the q=1 surface and zero outside. This displacement makes $\delta W = 0$ in (4.11). In the large aspect ratio tokamak, the region with $q_0 < 1$ is unstable to a resistive kink mode[17]. At low aspect ratio, this mode can be stable or unstable depending on the profiles.

Despite its simplicity, the tophat current profile enables us to draw pretty much the correct operational diagram for tokamaks. There are of course several comments to be made about this diagram. One such comment is that although it was commonly agreed for a long time that tokamaks usually operate with a central q very close to unity, there are experimental measurements of q_0 significantly below 1, e.g., $q_0 = 0.7$ has been reported from the TEXTOR tokamak[18]. This is in the region marked by a question mark in our large aspect ratio stability diagram. The MHD community is presently under the challange to explain how (and if!) $q_0 = 0.7$ can be consistent with the occurrence of sawtooth oscillations in the central temperature. These oscillations are induced by an m=1/n=1 displacement of the center, and it was previously thought that such an instability would occur as soon as q_0 becomes even slightly less than unity[19]. Although it is now understood that this is not necessarily the case at small aspect ratio, the sawtooth presently pose many questions for which we do not have answers. Here is an important problem that is as yet unresolved!

For the purpose of these lectures, the most important comment is that we found stability for modes with a resonant surface in the plasma, simply by imposing the requirement that $\psi_{m,n} = 0$ at the resonant surface $q = m/n$. If we had treated the region at q=m/n as a vacuum, we could have found instability. Thus, if there is conducting plasma at the resonant surface, the plasma is stable, if there is vacuum, it may be unstable! The stabilization occurs because the magnetic field is frozen into the plasma, which forces ψ to vanish at the resonant surface. This stabilization is lost if the resonant surface is in a vacuum or if the plasma is not perfectly conducting. The case of imperfectly conducting plasma leads to the resistive tearing modes, so called because they tear the magnetic field lines because of finite resistivity. This is the subject of the next section.

5. RESISTIVE TEARING MODES

The relevance of resistive MHD modes to the stability of magnetic confinement devices was recognized around 1960 and the first systematic study of the subject was given by Furth, Killeen and Rosenbluth in a famous paper usually referred to as FKR[20]. The tearing mode is a global mode like the external kink mode, but the dynamics are concentrated to a thin layer

around the resonant surface where the field lines are torn by finite resistivity, allowing a nonzero ψ even though $F = 0$. The tearing mode has a growthrate that is a fractional power of the Alfvén τ_A and the resistive diffusion time $\tau_R = a^2\mu_0/\eta$. The ratio $S = \tau_R/\tau_A$ is called the Lundquist number and is very large in present-day tokamaks, $S > 10^8$ in JET, for example. The growth-rate of the resistive tearing mode is of the order $\tau_A^{-2/5}\tau_R^{-3/5}$, which is very slow in comparison with ideal instabilities, whose growthrates are of the order τ_A^{-1}. The growthrate of the resistive kink mode[17] is of the order $\tau_A^{-2/3}\tau_R^{-1/3}$, i.e., intermediate between the resistive tearing and ideal modes.

First of all, we introduce a resistive electric field in the flux equation (3.3)

$$\frac{\partial \mathbf{A}}{\partial t} = \mathbf{v} \times \mathbf{B} - \eta \mathbf{J} + \nabla V \tag{5.1}$$

In the large aspect ratio ordering, we have $J_z >> J_\perp$ so this term goes easily through the derivation of Sec. 3 and we have in place of (3.10)

$$\rho \left(\frac{\partial}{\partial t} + \mathbf{v}_\perp \cdot \nabla\right) \omega = \mathbf{B} \cdot \nabla j \tag{5.2a}$$

$$\frac{\partial \psi}{\partial t} = \mathbf{B} \cdot \nabla \phi - \eta j \tag{5.2b}$$

Linearization of this system is straightforward; (4.2) is replaced by

$$\begin{aligned} \gamma\psi &= F\phi + \eta\nabla_\perp^2\psi \\ -\rho\gamma\nabla_\perp^2\phi &= F\nabla_\perp^2\psi - \frac{m}{r}\frac{dj_0}{dr}\psi \end{aligned} \tag{5.3}$$

In (5.3) we consider time-dependence $e^{\gamma t}$ and a factor i has been absorbed in ϕ. FKR found that outside the thin layer near F=0, the solutions of (5.3) are close to force balance and can be obtained by setting the inertial term in (5.3) to zero

$$\frac{1}{r}\frac{d}{dr}r\frac{d\psi}{dr} - \frac{m^2}{r^2}\psi - \frac{m}{B_\theta(m-nq)}\frac{dj_0}{dr}\psi = 0 \tag{5.4}$$

We note that this is the Euler-Lagrange equation for ψ in the ideal case. This equation holds to a good approximation sufficiently far away from the resonant surface and its solution will be referred to as the external solution ψ_{ext}. In the vicinity of the resonant surface, in the resistive layer, both the resistive and inertial terms in (5.3) become important. However, because the layer is thin, it is only necessary to keep track of the highest derivatives with respect to r.

Furthermore, since F = 0 at the resonant surface $r = r_S$, we can set $F \approx F'x$ with $x = r - r_S$. Thus, the equations to be solved in the layer are

$$\gamma\psi = F'x\phi + \eta \frac{d^2\psi}{dx^2} \tag{5.5a}$$

$$-\rho\gamma \frac{d^2\phi}{dx^2} = F'x \frac{d^2\psi}{dx^2} - F''\psi \tag{5.5b}$$

where F" stands for $(m/r)\, dj_0/dr$, which is really equal to $F'' - 3F'/r$ in cylindrical geometry. (This somewhat confusing notation is used to make the connection to the standard procedure of considering the tearing mode in planar geometry, and also saves some space.) What is needed is to solve the external and resistive layer equations separately and finally match the solutions. The matching condition will determine the growthrate of the mode.

Before carrying out this program in detail, we consider for a moment how may even be possible to match a fourth order equation (5.5) to a second order equation (5.4). The fourth order system needs two extra constants of integration; where do they come from ? To see that we can simply consider the local properties of (5.5), setting $d/dx = ik_x$, and obtain the local "dispersion relation"

$$\rho\gamma\eta k_x^4 + (F'^2x^2 + \rho\gamma^2)\, k_x^2 + xF'F'' = 0$$

In the limit of small resistivity, the coefficient for k_x^4 is very small, and thus the two roots can be approximated as

$$k_x^2 \approx - xF'F''/(F'^2x^2 + \rho\gamma^2) \tag{5.6a}$$

$$k_x^2 \approx - (F'^2x^2 + \rho\gamma^2)/\rho\gamma\eta \tag{5.6b}$$

The solution (5.6a) behaves in the same way as the solution of the external equation for large |x|, but the other solution (5.6b) grows/decays for large |x| as $\exp(\pm F'x^2/2(\rho\gamma\eta)^{1/2})$, i.e., very rapidly in the limit of small resistivity. We get the two extra constants of integration by requiring that the exponentially large components corresponding to (5.6b) vanish for large |x|. That is necessary in order for the solution of the inner layer problem (5.5) to match to the external solution. It means that we discard any solution where ψ is much larger outside the layer than within it. Thus, we admit that the solution of the layer equations (5.5) is rapidly varying inside the layer, but the rapid variation must decay rather than grow away from the layer.

A. Formulation of the boundary layer problem

It is useful to consider the nature of the external solution to see what conditions are required in order for the internal solution to match to it. There is a singularity of the external equation if $dj_0/dr \neq 0$, but this only gives an x log|x| singularity of the solution

$$\psi_{ext} \approx A \left[1 + \frac{F''}{F'} (x \log|x| - x) \right] + Bx + O(x^2) \tag{5.7}$$

Thus, if the thickness δ of the layer is small, we anticipate that the inner solution will be nearly constant in the layer $\psi_{inner} = \psi_{ext}(r_S) + O(\delta\log\delta) \approx \psi_{ext}(r_S)$. This is referred to as the "constant-ψ approximation". It is justified when ψ_{ext} is almost constant in the layer, which is the case in the limit of small resistivity for the resistive tearing mode (but not for the resistive kink mode).

Thus, the matching must be done to an external solution for ψ that is continuous at the resonant surface. However, if ψ_{ext} is continuous, there will in general be a jump in $d\psi_{ext}/dr$, and this jump is connected to the total current in the layer. Equating the jump in derivative for the internal and external ψ, we have the matching condition

$$\Delta'_{ext} = \Delta'_{int} \tag{5.8a}$$

where

$$\Delta'_{ext} = \lim_{\delta \to 0^+} \left[\psi'_{ext}(r_S+\delta) - \psi'_{ext}(r_S-\delta) \right] / \psi_{ext}(r_S) \tag{5.8b}$$

$$\Delta'_{int} = \lim_{X/\delta \to +\infty} \psi_{int}^{-1}(0) \int_{-X}^{X} \frac{d^2\psi_{int}}{dx^2}\, dx = \frac{1}{\eta\psi} P \int_{-\infty}^{\infty} (\gamma\psi - F'x\phi_{int})\, dx \tag{5.8c}$$

and where P denotes principal value. Two comments need to be made about Eqs. (5.8). First because the layer has a very small width δ, and ψ' is determined essentially by the external solution, ψ and its derivatives scale the following way with δ; $\psi = \text{const} + O(\delta)$, $\psi' = O(1)$ and $\psi'' = O(1/\delta)$. Therefore, ψ can be approximated as a constant but its derivatives cannot. Second, the principal values in (5.8b,c) are needed because, as can be seen from (5.7)

$$\psi'_{ext}/\psi_{ext}(r_S) \approx (F''/F') \log|x|$$

so that $d\psi_{ext}/dr(r_s \pm \delta)$ both diverge logarithmically for small δ, just as $d\psi_{int}/dx(\pm X)$ diverge logarithmically for large X/δ.

Thus, the procedure for solving the resistive MHD problem (5.2) in the limit of small resistivity is

I. Solve the external equation (5.4) separately on both sides of the resonant surface and compute Δ'_{ext}

II. Solve the inner layer problem (5.5) for an assumed value of γ and compute $\Delta'_{int}(\gamma)$

III. Finally, set $\Delta'_{int}(\gamma) = \Delta'_{ext}$, which determines γ

Introducing the constant-ψ approximation in (5.5) and eliminating $d^2\psi/dx^2$, we obtain a second order equation for ϕ

$$\rho\gamma\eta \frac{d^2\phi}{dx^2} - F'^2x^2 \phi = (\eta F'' - F'x\gamma) \psi \qquad (5.9)$$

The solution of (5.9) is to be substituted into the matching condition

$$\Delta'_{ext} = \frac{1}{\eta\psi} P \int_{-\infty}^{\infty} (\gamma\psi - F'x\phi)\, dx \qquad (5.10)$$

From (5.9) and (5.10), we can estimate the time and space-scales involved without a detailed calculation. (5.9) shows that the characteristic length (the width of the tearing layer) is $\delta = (\rho\gamma\eta/F'^2)^{1/4}$. The integrand in (5.10) is peaked over a distance δ and has a maximum value of order $\gamma\psi$. Thus, $\Delta' \approx \delta\gamma/\eta$, which, together with the estimate for δ gives

$$\gamma \sim \Delta'^{4/5}\, \eta^{3/5}\, \rho^{-1/5}\, F'^{2/5}$$

$$\delta \sim \Delta'^{1/5}\, \eta^{2/5}\, \rho^{1/5}\, F'^{-2/5}$$

B. Solution by Fourier transformation

There are several different ways to solve Eq. (5.9). FKR used an expansion in Hermite functions. The method of Fourier transformation reduces the amount of algebra involved and is applicable to a variety of similar problems[21]. We define the Fourier transform $\Phi(k)$ as

$$\Phi(k) = \int_{-\infty}^{\infty} \phi(x)\, e^{-ikx}\, dx \quad , \quad \phi(x) = \int_{-\infty}^{\infty} \Phi(k)\, e^{ikx}\, \frac{dk}{2\pi} \qquad (5.11)$$

and write $\Phi(k) = FT[\phi(x)]$. The Fourier transformed Eq. (5.9) becomes

$$\frac{d^2\Phi}{dk^2} - \frac{\rho\gamma\eta}{F'^2} k^2 \Phi = \frac{2\pi}{F'} [\, \eta \frac{F''}{F'} \delta(k) - i\gamma \delta'(k)\,] \psi \qquad (5.12)$$

where $\delta(k)$ denotes the Dirac delta function[22]. Note that the homogeneous part of the equation did not change in form under the Fourier transformation. The advantage of working in Fourier space is that in the Fourier transformed equation (5.12), the sources are entirely localized at $k=0$. The desired solution of (5.12) is easily constructed from the two unique solutions Φ_+ and Φ_- of the homogeneous equation that decay as $k \to \pm\infty$ on the real axis. We set $\Phi = A_+\Phi_+$ for $k > 0$ and $\Phi = A_-\Phi_-$ for $k < 0$ and adjust the coefficients so as to produce the correct source term at $k = 0$ in (5.12). This source term leads to the following jump conditions for Φ

$$\Phi(0^+) - \Phi(0^-) = -\frac{2\pi i\gamma}{F'} \psi \qquad (5.13a)$$

$$\frac{d\Phi}{dk}(0^+) - \frac{d\Phi}{dk}(0^-) = \frac{2\pi\eta F''}{F'^2} \psi \qquad (5.13b)$$

It is convenient to transform also the Δ' condition (5.10) to Fourier space, which gives

$$\Delta' = -\frac{iF'}{2\eta\psi} [\, \frac{d\Phi}{dk}(0^+) + \frac{d\Phi}{dk}(0^-)\,] \qquad (5.14)$$

This expression follows from (5.9) because the integral can be interpreted as the value at $k = 0$ of

$$FT [\, \gamma\psi - F'x\phi\,] = 2\pi\gamma\psi\, \delta(k) - iF' \frac{d\Phi}{dk} \qquad (5.15)$$

The $\delta(k)$ originating from the $\partial\psi/\partial t$-term in (5.15) is exactly cancelled by the $d\Phi/dk$ term with the jump in (5.13a). However, even with the δ-function removed, $d\Phi/dk$ is not well defined at $k = 0$ because of the jump (5.13b). It can be shown rigorously in this case, that the procedure of taking the principal value in (5.10) corresponds to taking the average of $d\Phi/dk(0^+)$ and $d\Phi/dk\,(0^-)$ in Fourier space. Combining (5.13b) and (5.14) we get

$$\frac{d\Phi}{dk}(0^\pm) = \frac{i\eta}{F'} \psi\, (\Delta' \mp \frac{i\pi F''}{F'}) \qquad (5.16)$$

which gives the normalization condition for $\Phi(k)$. To calculate $\Phi(k)$, we use the two solutions of the homogeneous (5.12)

$$\frac{d^2\Phi}{dk^2} - \frac{\rho\gamma\eta}{F'^2} k^2 \Phi = 0 \tag{5.17}$$

such that $\Phi(k) \to 0$ as $k \to +\infty$ and $k \to -\infty$, respectively, and then adjust the normalization according to (5.16). Substituting (5.16) in (5.13a) finally gives the eigenvalue condition

$$\left(\Delta' + \frac{i\pi F''}{F'} \right) \frac{\Phi(0^-)}{d\Phi/dk(0^-)} - \left(\Delta' - \frac{i\pi F''}{F'} \right) \frac{\Phi(0^+)}{d\Phi/dk(0^+)} = \frac{2\pi\gamma}{\eta} \tag{5.18}$$

Note that the solution of the homogeneous inner layer equation enters the eigenvalue relation exclusively via the logarithmic derivative at $k = 0^{\pm}$.

The solution of (5.17) that is well behaved as $k \to +\infty$ is

$$\Phi_+(k) = (k/k_0)^{1/2} K_{1/4}(k^2/2k_0^2)$$
$$k_0^4 = F'^2/\eta\rho\gamma \tag{5.19}$$

where K is the modified Bessel function of the second kind. The logarithmic derivative at $k = 0^+$ is easily found from an expansion of Φ for small k. It is sufficient to use

$$K_\nu(z) = \frac{\pi}{2 \sin \pi\nu} [\, I_{-\nu}(z) - I_\nu(z) \,]$$

$$I_\nu(z) = \frac{(z/2)^\nu}{\Gamma(\nu+1)} [\, 1 + O(z^2) \,]$$

which gives

$$\Phi_+(k) = \pi \left[\frac{1}{\Gamma(3/4)} - \frac{2k}{\Gamma(1/4)k_0} + O(k^2/k_0^2) \right]$$

Thus,

$$\frac{\Phi_+(0^+)}{d\Phi_+/dk(0^+)} = - k_0 \frac{\Gamma(1/4)}{2\Gamma(3/4)} = - \frac{\Phi_-(0^-)}{d\Phi_-/dk(0^-)} \tag{5.20}$$

where the last equality followed from the symmetry of (5.17), $\Phi_-(-k) = -\Phi_+(k)$. Using (5.20) in (5.18), we finally obtain

$$\gamma = \Delta'^{4/5} \eta^{3/5} \rho^{-1/5} F'^{2/5} \left(\frac{\Gamma(1/4)}{2\pi\,\Gamma(3/4)} \right)^{4/5}$$
$$\approx 0.55\, \Delta'^{4/5} \eta^{3/5} \rho^{-1/5} F'^{2/5} \tag{5.21}$$

This is the asymptotic expression for the growthrate of the resistive tearing mode in the limit of small resistivity.

In addition to the growth-rate, we can also give an expression for the inner-layer solution. Substituting $\Phi(k)$ into the Fourier integral gives

$$\phi(x) = \frac{\eta\Gamma(1/4)}{2\pi^2 F'} \psi \int_{-\infty}^{\infty} \left(\Delta' \sin kx - \frac{\pi F''}{F'} \cos kx \right) (k\, k_0)^{1/2} K_{1/4}(k^2/2k_0^2)\, dk \tag{5.22}$$

Thus, ϕ has one piece that is odd in x and proportional to Δ' and one piece that is even in x and proportional to F''/F', i.e., to the local current gradient.

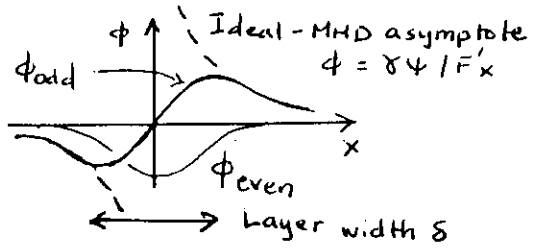

Figure 4. Qualitative plot of $\phi(x)$.

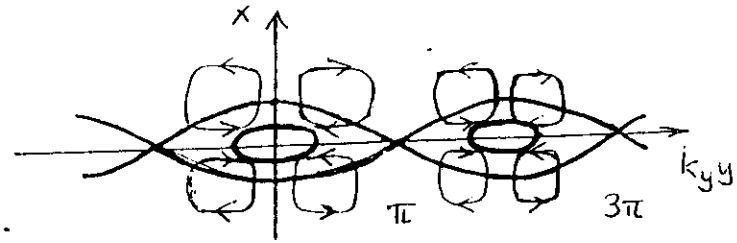

Figure 5. Field lines (heavy) and streamlines for the resistive tearing mode.

In x-y space the field lines (i.e., the level curves of the total flux function $\psi = \psi_0 + \psi_1$) and the stream lines (level curves of ϕ) for a case with no local current gradient look as shown in Fig. 5. Here the heavy lines are magnetic field lines. Note that an island is formed around the resonant surface and that the flow is pulling the field lines away from the O-points at x=0, $k_y y = 0, \pm 2\pi, \pm 4\pi, \ldots$ and in toward the X-points at $k_y y = \pm\pi, \pm 3\pi, \ldots$

D. Energy balance

The tearing mode is interesting from the point of view of energy balance. This is more complicated than in ideal MHD because of the dissipation. We start by considering the sum of the contributions of the mode to ohmic dissipation and the power being convected into kinetic energy

$$\frac{dW}{dt} = \int_{-\infty}^{\infty} (\eta j^2 + \rho\gamma\omega\phi)\, dx$$

In the thin layer approximation, the Fourier transforms of the perturbed vorticity and current density are

$$FT[\omega] = k^2 \Phi(k)$$

$$FT[j] = [iF' d\Phi/dk - 2\pi\gamma\psi\, \delta(k)]/\eta$$

i.e., FT[j] is the regular part of $d\Phi/dk$. By means of Parseval's theorem and the symmetry $\Phi(-k) = \Phi^*(k)$, the released power can be written as

$$\frac{dW}{dt} = \frac{1}{\pi}\int_{-\infty}^{\infty} \left(\frac{F'^2}{\eta}\left|\frac{d\Phi}{dk}\right|^2 + k^2\rho\gamma|\Phi|^2\right) dk = -\frac{F'^2}{\pi\eta}\Phi^*(0^+)\frac{d\Phi}{dk}(0^+) \qquad (5.23)$$

where we used a partial integration and Eq. (5.12). The energy released by the tearing mode is now obtained by dividing (5.23) by 2γ (the growth rate for a quadratic quantity)

$$W = \frac{1}{2}\psi_s^2\,[\,\Delta' + (\pi F''/F')^2/\Delta'] \qquad (5.24)$$

We note that the released energy has one piece proportional to Δ' and one related to the local current gradient. It can be shown that 1/4 of the energy goes into fluid motion and 3/4 into joule heating[21].

E. Other types of resistive modes

In addition to the tearing mode, FKR also discuss other types of resistive modes. The rippling mode is similar to the tearing mode but it is driven unstable by gradients in the resistivity and is almost independent of Δ'. It is generally agreed that the rippling mode is stable in high-temperature plasmas ($\geq$ 50 eV) because of high thermal conductivity along the fieldlines. The resistive g-mode is driven by pressure gradients in combination with unfavourable curvature, and its growth-rate scales like $\tau_A^{-2/3}\tau_R^{-1/3}$. This mode is stable in tokamaks with $q > 1$, where the curvature is favourable, however, it should be unstable in RFPs.

Coppi, Greene, and Johnson[23] solve the compressible resistive MHD problem in a cylinder with finite pressure. This work was extended to toroidal geometry by Glasser, Greene, and Johnson[24]. Coppi, Galvao, Pellat, Rosenbluth, and Rutherford[17] treated the resistive kink mode. This mode is at the transition between the resistive tearing mode and an ideal instability and cannot be treated by the constant-ψ approximation. Its growth rate scales as $\tau_A^{-2/3}\tau_R^{-1/3}$.

6. IMPLICATIONS OF TEARING MODES FOR TOKAMAKS

A. Linear stability

Equation (5.21) shows that the stability of the resistive tearing mode only depends on Δ'. The mode is stable if $\Delta' < 0$ and unstable if $\Delta' > 0$. Of the two external solutions shown here, (a) is unstable and (b) is stable.

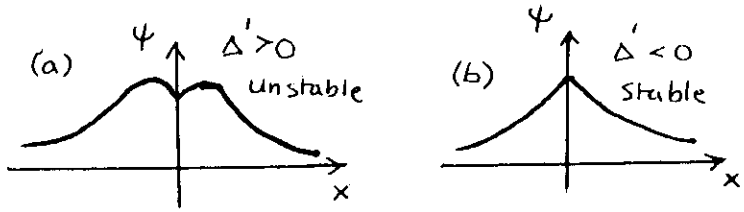

Figure 6. External solutions for ψ. (a) tearing unstable $\Delta' > 0$ and (b) tearing stable $\Delta' < 0$.

The Δ' criterion is easy to understand intuitively. At the resonant surface, the ideal MHD dynamics cannot change ψ, so ψ evolves in time only by resistive diffusion. It is clear that in

may well be compatible with transport effects, which appear to determine the current profiles. However, it is known experimentally that the current - or q_a-limit of tokamaks is $q_a \geq 2$, not 2.6. Cheng, Furth, and Boozer[26] showed that there are tearing-stable profiles for q_a between 2 and 2.6, but the stable profiles become increasingly distorted as q_a approaches 2. Such profiles would almost certainly not be compatible with transport effects. The resolution of this problem appears to be that for $q_a \leq 2.6$, tearing modes are quite strongly stabilized by the presence of a conducting wall. Contrary to the case of external kink modes, tearing modes can be stabilized by finitely conducting walls because, in practice, they have real frequencies, that are usually larger than the inverse of the wall time constant[27,28]. This rotation frequency is determined by the dynamics in the resistive layer. As this dynamics is slow, the tearing mode is almost frozen into the plasma at the resonant surface. Thus, if the plasma is rotating (even very slowly) the mode will be forced to rotate with the plasma. If this rotation is fast compared with the resistive decay time (L/R) of the wall, the mode will not be able to penetrate the wall and can therefore be wall stabilized.

When wall stabilization is accounted for, it is relatively easy to construct profiles that are stable to all tearing modes for q_a between 2 and 2.6 and $q_0 = 1$. When q_a drops below 2, the m=2/n=1 mode turns into a resistive kink, that cannot be stabilized by resistive walls. This appears to explain why the current limit is more or less exactly at $q_a = 2$.[28] It is the impression of the author that an important reason for the success of tokamaks is that the profiles which occur naturally as a result of transport tend to be MHD stable. The only obvious exception to this statement is the peaking of the current in the centre, which gives rise to the sawteeth. These, however, do not have a strongly detrimental effect on confinement at least not during high-q_a operation.

B. Nonlinear evolution of a single unstable tearing mode

In this section, we briefly discuss some theoretical and computational results concerning the nonlinear evolution of tearing modes. When the tearing mode grows, it leads to the formation of a magnetic island at the resonant surface.

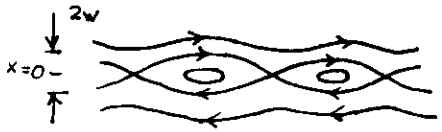

Figure 7. Magnetic island caused a nonlinear tearing mode.

Rutherford[29] showed that the growth of the tearing mode slows down once the mode becomes nonlinear, which occurs when the width w of the island is comparable to the width δ of the linear resistive layer.

In somewhat simplified terms, Rutherford's argument is as follows. In the region inside the island $|x| < w$, the perturbed ψ cannot grow by the ideal MHD mechanism but only by the resistive electric field. Thus the perturbed magnetic flux evolves according to

$$\partial\psi/\partial t = -\eta j \tag{6.2}$$

When the island has reached a width $w > \delta$, the matching to the external solution must be done an island width away from the resonant surface, rather that the linear tearing with δ. Thus, the perturbed current density, which is about uniform across the island is given by

$$j = -[\psi'(+w) - \psi'(-w)]/w = -\psi\Delta'/w \tag{6.3}$$

where Δ' is now defined for the external solution with respect to $r_s \pm w$. Combining (6.2) and (6.3) we have

$$\partial\psi/\partial t = \psi\eta\Delta'/w \tag{6.4}$$

where it can be seen that w replaces δ in linear theory. It is easy to show that the island width is proportional to the square root of the perturbation in ψ. This, together with (6.4), gives

$$\frac{dw}{dt} = w\,\frac{dw}{w\,dt} = \frac{w}{2}\,\frac{d\psi}{\psi\,dt} = \frac{1}{2}\,\eta\Delta' \tag{6.5}$$

Equation (6.5) shows that the island grows linearly in time at a rate proportinal to $\eta \propto \tau_R^{-1}$, i.e., on the slow resistive time-scale. White et al[30] showed that $m > 1$ modes saturate when the island grows sufficiently large to affect the equilibrium current profile so that Δ' decreases to zero. For specially chosen profiles[31] with q_0 far above 1 (but less than 2) and a sharp current gradient inside the q=2 surface, the magnetic island resulting from the m=2/n=1 resistive tearing mode can become very large.

C. Major disruption

It seems appropriate to say a few words in the final section of these lecture notes about experimental consequences of tearing modes. It is well known from experiments, see e.g.[32], that an m=2/n=1 mode plays a dominant role in major disruptions which lead to the complete and violent termination of a discharge. There are several types of disruption, notably, current-density- and β-limit disruption and current ramp disruption. Each type is caused by a different way of violating MHD stability. The disruptions that give the most important limitations for the operation of a tokamak are the current and density limit disruptions. The current limit in near-circular machines is $q_a = 2$, and for $q_a < 2$, an m=2/n=1 external kink mode becomes unstable and leads to disruption with a very short precursor. The density limit is empirically known to be $n < CB_T/Rq_a$, where C is a weakly machine-dependent number between 1×10^{20} and 2×10^{20} Wb^{-1} for ohmically heated tokamaks. The two requirements $q_a > 2$ and $n < CB_T/Rq_a$ restrict the operating regime to a triangle in the Hugill diagram, where the normalized density nR/B_T is plotted versus the normalized current $1/q_a$.

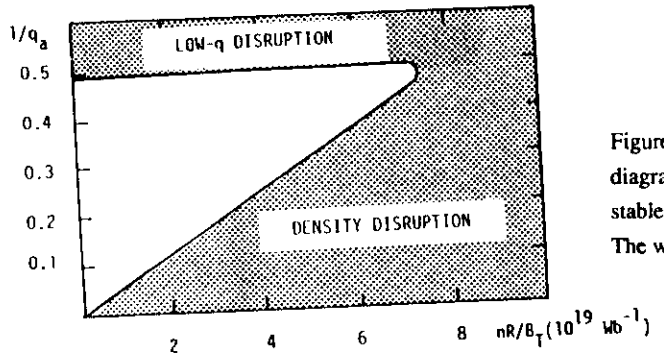

Figure 8. Schematic Hugill diagram showing boundaries stable tokamak operation. The white region is stable.

In the initial phase of a density limit disruption, the outer parts of the plasma are cooled by radiation losses exceeding the total heating power. As a consequence, the current channel contracts and when the current density becomes sufficiently low at the q=2 surface, the m=2/n=1 tearing mode goes unstable. If this were the only mode to become unstable, the contraction might not be so serious, the plasma would just develop a magnetic island at the q=2 surface. However, experimental observations show that the ensuing MHD activity can be extremely violent, and finally leads to the complete loss of plasma pressure and current.

Waddell et al[33] showed by numerical simulation that very dramatic, nonlinear interactions and destructive MHD activity results if the m=2/n=1 and m=3/n=2 tearing modes are both unstable, and that the growth of the 3/2 mode can be enhanced in the presence of the 2/1 mode. The simultaneous presence of large amplitude tearing modes with different helicity

m/n not only leads to violent MHD activity, but also breaks up the magnetic surfaces, and causes the magnetic field lines to become stochastic over some part of the cross-section. This means that the electrons can follow a magnetic field line over a large radial distance, and therefore energy confinement is severely deteriorated. It seems clear that such nonlinear interactions of tearing modes are responsible for the early phase of a density disruption, when repeated minor disruptions occur. These minor disruptions involve violent MHD activity and lead to partial, but not complete loss of the plasma energy, but do not quench the current.

A more recent simulation study[34], in which it was attempted to simulate density disruptions in a self-consistent way, by slowly changing the external conditions of the plasma (rather than starting the simulation with a highly unstable equilibrium), showed a sequence of minor disruptions, similar to observations in, e.g., JET. Once the 2/1 mode grows to sufficient amplitude in these simulations, it modifies the current gradient in such a way that the current gradient inside q = 3/2 is increased. As a consequence, the 3/2 mode is driven unstable and creates an island which, in its turn, modifies the current gradient to make the 4/3 mode unstable, etc. This successive destabilization of resistive modes takes the form of a front moving inward from the q=2 surface. Behind the front, the magnetic field has become turbulent and stochastic (i.e., the magnetic surfaces have been destroyed by the simultaneous presence of modes with different helicities m/n). Figure 9 shows the current and temperature distribution in a poloidal cross-section during the inward propagation of such a front. Note the clear separation between the laminar region ahead of the front and the turbulent region behind it.

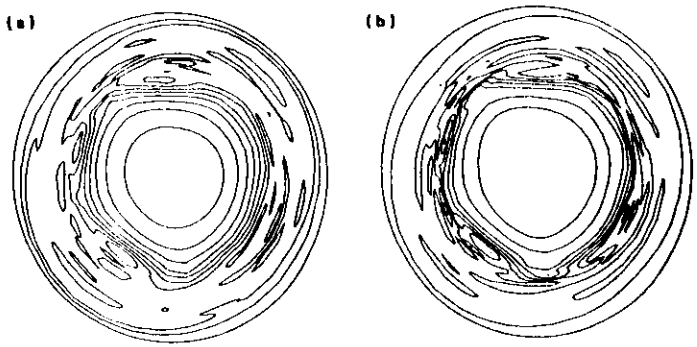

Figure 9. Level curves of (a) plasma temperature and (b) current density during a minor disruption (from Ref. 34)

When the front reaches the $q = 1$ region, the current distribution is similar to a top-hat with $q = 1$ in the center. At this point, the front stops, simply because there is no longer any driving energy for a linear instability. The simulation described in Ref. 34 showed several such events of fronts propagating from the $q=2$ surface toward the central region, similar to the "minor disruptions" that occur in the early phase of density limit disruptions. These destroy the confinement in the region $1 < q \leq 2$, but do not quench the plasma current. In a major disruption, the minor disruptions are followed by a very fast drop in the plasma temperature, the socalled energy quench. After this, the plasma current starts to decay, and the plasma is lost. Different explanations for the energy quench have been proposed[32,35], but sofar, the final phase of a major disruption remains poorly understood theoretically. A more extensive review of theories and simulations of major disruptions is given in Ref. 35.

REFERENCES

1. J.A. Tataronis and W. Grossman, Nucl. Fusion **16**, 667 (1976).
2. D. Dobrott and J.M. Greene, Phys. Fluids **13**, 2391 (1970).
3. A. Bondeson and R. Iacono, Phys. Fluids (to appear July 1989).
4. J. Freidberg, Rev. Mod. Phys. **54**, 801 (1982).
5. L. Woltjer, Proc. Nat. Acad. Sci **44**, 489 (1958).
6. J.B. Taylor, Phys. Rev. Lett. **33**, 1139 (1974).
7. D.C. Robinson, Plasma Phys. **13**, 439 (1971).
8. M.N. Rosenbluth and M.N. Bussac, Nucl. Fusion **19**, 489 (1979).
9. F. Troyon, R. Gruber, H. Saurenmann, S. Semenzato, and S. Succi, Plasma Phys. and Controlled Fusion **26**, 209 (1984).
10. H. Strauss, Phys. Fluids **19**, 135 (1976).
11. I.B. Bernstein, E.A. Frieman, M.D. Kruskal, and R.M. Kulsrud, Proc. R. Soc. London, Ser. A **244**, 17 (1958).
12. H. Strauss, Phys. Fluids 20, 1354 (1977).
13. J.F. Drake and T.M. Antonsen, Phys. Fluids **27**, 898 (1984).
14. R. Izzo, D.A. Monticello, J. DeLucia, W. Park, and C.M. Ryu, Phys. Fluids **28**, 903 (1985).
15. E.K. Maschke and J. Morras Tosas, Plasma Phys. and Controlled Fusion **31**, 563 (1989); J. Morros Tosas, PhD Thesis, Université de Provence (1989).
16. V.D. Shafranov, Sov. Phys. - Tech. Phys. **15**, 175 (1970).
17. B. Coppi, R. Galvao, R. Pellat, M. Rosenbluth, and P. Rutherford, Sov. J. Plasma Phys. **2**, 533 (1976).
18. H. Soltwish, W. Stodiek, J. Manickam, and J. Schluter, in Plasma Phys. and Controlled Nuclear Fusion Research 1986 (IAEA, Vienna, 1987) Vol 1, p 263.
19. B.B. Kadomtsev, Sov. J. Plasma Phys. **1**, 389 (1975).
20. H.P. Furth, J. Killeen, and M.N. Rosenbluth, Phys. Fluids **6**, 459 (1963).
21. A. Bondeson and J.R. Sobel, Phys. Fluids **27**, 2028 (1984); A. Bondeson and M. Persson, Phys. Fluids **29**, 2997 (1986).
22. M.J. Lighthill, *Introduction to Fourier Analysis and Generalized Functions* (Camebridge University Press, Camebridge, 1958).
23. B. Coppi, J.M. Greene, and J.L. Johnson, Nucl. Fusion **6**, 101 (1966); see also J.L. Johnson, J.M. Greene, and B. Coppi, Phys. Fluids **6**, 1169 (1963).
24. A.H. Glasser, J.M. Greene, and J.L. Johnson, Phys. Fluids **18**, 875 (1975); ibid. **19**, 567 (1976).
25. A.H. Glasser, H.P. Furth, and P.H. Rutherford, Phys. Rev. Lett. **38**, 234 (1977).
26. C.Z. Cheng, H.P. Furth, and A.H. Boozer, Plasma Phys. and Controlled Fusion **29**, 351 (1987).
27. M.F.F. Nave and J.A. Wesson, in Controlled Fusion and Plasma Physics (Proc. 14th Eur. Conf, Madrid, 1987), Vol 11D, Part III, p1103.
28. A. Bondeson and M. Persson, Nucl. Fusion **28**, 1887 (1988).
29. P.H. Rutherford, Phys. Fluids **16**, 1903 (1973).
30. R.B. White, D.A. Monticello, M.N. Rosenbluth, and B.V. Waddell, Phys. Fluids **20**, 800 (1977).
31. R.B. White, D.A. Monticello, and M.N. Rosenbluth, Phys. Rev. Lett. **39**, 1618 (1977); J.F. Drake and R.G. Kleva, Phys. Rev. Lett. **53**, 1465 (1984).
32. J.A. Wesson, et al, Nucl. Fusion **29**, 641 (1989).
33. B.V. Waddell, B. Carreras, H.R. Hicks, and J.A. Holmes, Phys. Fluids **22**, 896 (1979).
34. A. Bondeson, Nucl. Fusion **26**, 929 (1986).
35. A. Bondeson, in Theory of Fusion Plasmas, (Proc. Workshop Varenna, 1987), Editrice Compositori, Bologna (1988) p. 325.